THE JOURNAL OF BIOLOGICAL CHEMISTRY
Vol. 279, No. 53, Issue of December 31, pp. 55644–55650, 2004

*Printed in U.S.A.*

# Structural Evidence That the 32-Kilodalton Lipoprotein (Tp32) of *Treponema pallidum* Is an L-Methionine-binding Protein*

Received for publication, August 12, 2004, and in revised form, October 13, 2004
Published, JBC Papers in Press, October 15, 2004, DOI 10.1074/jbc.M409263200

**Ranjit K. Deka‡, Lori Neil‡, Kayla E. Hagman‡, Mischa Machius§, Diana R. Tomchick§, Chad A. Brautigam§, and Michael V. Norgard‡¶**

*From the Departments of ‡Microbiology and §Biochemistry, University of Texas Southwestern Medical Center, Dallas, Texas 75390*

**A structure-to-function approach was undertaken to gain insights into the potential function of the 32-kDa membrane lipoprotein (Tp32) of *Treponema pallidum*, the syphilis bacterium. The crystal structure of rTp32 (determined at a resolution of 1.85 Å) shows that the organization of rTp32 is similar to other periplasmic ligand-binding proteins (PLBPs), in that it consists of two $\alpha/\beta$ domains, linked by two crossovers, with a binding pocket between them. In the pocket, a molecule of L-methionine was detected in the electron density map. Residues from both domains interact with the ligand. One of the crossover regions is comprised of a $3_{10}$-helix, a feature not typical in other ligand-binding proteins. Sequence comparison shows strong similarity to other hypothetical methionine-binding proteins. Together, the data support the notion that rTp32 is a component of a periplasmic methionine uptake transporter system in *T. pallidum*.**

Although syphilis is one of the oldest recognized sexually transmitted diseases, it remains among the most poorly understood. This primarily is a consequence of the fact that the etiological agent, *Treponema pallidum*, cannot be cultivated continuously *in vitro* (1). Hence, classical approaches for discerning *T. pallidum* membrane biology, which could reveal key aspects of its enigmatic parasitic strategy, are largely constrained (2, 3).

It is now generally accepted that lipoproteins are important integral membrane proteins of *T. pallidum* (4, 5); in fact, lipoproteins represent about 3% of the total coding capacity of the treponemal genome (6). In other bacteria, lipoproteins have importance as virulence factors, modular components of ATP-binding cassette (ABC)[1] transporters, receptors, protective immune targets, and pro-inflammatory agonists that contribute significantly to innate immune responses (5, 7–13). However, with one exception (9, 14), existing gene sequences and/or BLAST search information have not been fruitful for predicting the functions of treponemal lipoproteins. As an alternative approach to understanding the peculiar membrane biology of *T. pallidum* (2, 3, 15), we recently embarked on a structural biology initiative that seeks to garner structural insights into putative functions for a number of the *T. pallidum* membrane lipoproteins.

To this end, x-ray crystallographic studies were performed on Tp32 (gene number Tp0821). In the course of these studies, L-methionine was detected within a putative ligand-binding protein-like cleft. This has led us to conclude that Tp32 likely serves as a periplasmic receptor for L-methionine, probably lipid-linked to the outer leaflet of the *T. pallidum* cytoplasmic membrane. These findings add to our knowledge of the functions of treponemal membrane lipoproteins. The importance of Tp32 as a receptor for L-methionine, as well as its unique features, is discussed.

## EXPERIMENTAL PROCEDURES

*Construction of $His_6$-tagged rTp32*—To create a non-lipidated version of recombinant Tp32 (rTp32) in *Escherichia coli,* a fragment encoding amino acids 2–245 (residue 1 is the post-translationally modified N-terminal cysteine) was amplified by PCR using a genomic DNA template isolated from *T. pallidum*. The PCR primers were 5′-acgc**GGATCC**ACTCAGGTGAAGGATGAAACGGTGG-3′ and 5′-atcc**AAGCTT**TTACAAAGCAGGCGCCACCTCC-3′. The forward primer contained both an acgc overhang and a BamHI site (bold); the reverse primer contained an atcc overhang and a HindIII site (bold). PCR was performed using *TaKaRa Ex Taq* DNA polymerase with an annealing temperature of 55 °C. The amplification product was directionally cloned into the pProEX HTb vector (Invitrogen) that adds an N-terminal $His_6$ tag followed by a Tobacco Etch Virus protease cleavage site. Ligations were transformed into *E. coli* XL1-Blue competent cells (Stratagene), and colonies that tested positive by restriction digest were sequenced for verification.

*Expression and Purification of rTp32—E. coli* XL1-Blue containing the cloned *tp32* gene fusion was grown at 37 °C in LB medium containing 100 $\mu$g/ml of ampicillin until the cell density reached an $OD_{600}$ of 0.6. The culture was then shifted to 30 °C and induced for 5 h with 600 $\mu$M isopropyl-1-thio-$\beta$-D-galactopyranoside. Cells were harvested by centrifugation and lysed at room temperature for 30 min using 50 ml/liter culture of B-PER II (Pierce). The resulting suspension was spun at 27,000 × *g* for 15 min to pellet the cell debris. rTp32 was isolated from the supernatant by immobilization on a $Ni^{2+}$-affinity column and was eluted using 20 mM Tris-HCl (pH 8.5), 200 mM NaCl, 200 mM imidazole. Protein buffer was exchanged with 20 mM Hepes (pH 7.5), 100 mM NaCl, 15 mM $\beta$-mercaptoethanol, 2 mM octyl-$\beta$-glucoside (buffer A) by ultrafiltration using an Amicon device with a 10,000 molecular

* This work was supported by Grant AI-56305 from the NIAID, National Institutes of Health. Use of the Argonne National Laboratory Structural Biology Center beamlines at the Advanced Photon Source was supported by the United State Department of Energy, Office of Energy Research, under contract number W-31-109-ENG-38. The costs of publication of this article were defrayed in part by the payment of page charges. This article must therefore be hereby marked "*advertisement*" in accordance with 18 U.S.C. Section 1734 solely to indicate this fact.

*The atomic coordinates and structure factors (code 1XS5) have been deposited in the Protein Data Bank, Research Collaboratory for Structural Bioinformatics, Rutgers University, New Brunswick, NJ (http://www.rcsb.org/).*

¶ To whom correspondence should be addressed: Dept. of Microbiology, U.T. Southwestern Medical Center, 6000 Harry Hines Blvd., Dallas, TX 75390. Tel.: 214-648-5900; Fax: 214-648-5905; E-mail: michael.norgard@utsouthwestern.edu.

[1] The abbreviations used are: ABC, ATP-binding cassette; ESI-MS, electrospray ionization-mass spectrometry; HSQC, heteronuclear single quantum coherence; LAOBP, lysine-, arginine-, ornithine-binding protein; QBP, glutamine-binding protein; MUT, methionine uptake transporter; PLBPs, periplasmic ligand-binding proteins; r.m.s., root mean square.

weight (MW) size exclusion. The concentrated protein was then applied to a HiLoad 16/60 Superdex 75 gel filtration column that was pre-equilibrated in buffer A, using an Äkta fast performance liquid chromatography (FPLC) system (Amersham Biosciences). The column was run at a flow rate of 0.2 ml/min. Subsequent to elution, peak fractions were analyzed by SDS-PAGE. At this stage, protein was pure to apparent homogeneity (*i.e.* >95%). Fractions containing purified rTp32 were pooled and concentrated in buffer A to 30–35 mg/ml for crystallization. The oligomeric state of the purified protein was determined by size exclusion chromatography, using a calibration curve made with protein standards (Amersham Biosciences). For the production of selenomethionine (SeMet)-labeled protein, the expression vector was transformed into the methionine auxotroph *E. coli* B834 (Novagen) and grown in the presence of LB and 95% M9 medium supplemented with 125 mg/liter each of adenine, uracil, thymine, and guanosine nucleotide, 2.5 mg/liter thiamine, 4 mg/liter D-biotin, 20 mM glucose, 2 mM $MgSO_4$, 50 mg/liter each of 19 L-amino acids (excluding methionine), and 50 mg/liter L-selenomethionine (Sigma). For $^{15}N/^{13}C$-Met incorporation, *E. coli* containing the expression vector was grown in M9 minimal medium supplemented with 1 mg/liter of $^{15}NH_4Cl$ (Cambridge Isotope Laboratory) as the sole nitrogen source and 1 mM L-methionine-methyl-$^{13}C$ (Sigma).

Protein concentration was estimated from a molar extinction coefficient at 280 nm (16). The molecular weight of rTp32 was determined by electrospray ionization-mass spectrometry (ESI-MS). Protein N-terminal sequencing was performed by Edman degradation in an Applied Biosystem Model 494 automated protein sequencer. Proteomics and sequence analysis tools, available at the ExPASy proteomics server (us.expasy.org), were used for protein sequence analysis.

*Preparation of Apoprotein and NMR Spectroscopy*—For the production of ligand-free rTp32, purified protein was denatured at room temperature for 48 h in buffer A containing 6 M guanidine-HCl. Unbound ligand was removed by ultrafiltration in an Amicon-stirred cell using a 10,000 MW size exclusion filter and exhaustive washing with 500 ml of the above buffer. Protein was renatured by dilution into 1 liter of buffer A at a rate of 0.1 ml/min. After renaturation, residual insoluble protein was removed from the soluble refolded protein by centrifugation at 12,000 × *g* for 20 min. The renatured protein was further purified by gel filtration chromatography (as described above) and concentrated for NMR spectroscopy. All NMR experiments were performed on a Varian INOVA 500 MHz spectrometer, using NMRPipe (17) for data processing and NMRView (18) for analysis. Unless otherwise noted, data were collected on 500 μM samples in buffer A at 25 °C.

*Protein Crystallization and Structure Determination*—Wild-type rTp32 was crystallized by hanging-drop vapor diffusion (24) using 24-well Linbro plates (Hampton Research). Index crystallization kits (Hampton Research) were used to screen preliminary conditions. 62 of 96 droplets yielded crystals. The best crystals of rTp32 were routinely obtained with drops containing 5 μl of protein at a concentration of 35 mg/ml in buffer A and 5 μl of 0.4 M succinic acid (pH 7.0) at 20 °C. Crystals of a SeMet variant of rTp32 were generated under the same conditions. Crystals developed in 2–4 days. In order to cryoprotect a crystal, a solution of 0.4 M succinic acid and 2,3-butanediol was added to the crystal mother liquor, such that the final concentration of the 2,3-butanediol was 15%(v/v). Crystals so treated were transferred to a solution of 0.5 M succinic acid and 15% (v/v) 2,3-butanediol, then flash-cooled in liquid propane and subsequently stored under liquid nitrogen. Diffraction data were collected at 100 K using synchrotron radiation from beamline 19-ID of the Structural Biology Center at the Advanced Photon Source (Argonne National Laboratory). The diffraction data were indexed, integrated, and scaled in the HKL2000 program package (19). Data sets were taken on a crystal of the SeMet variant of rTp32 to a maximum Bragg spacing ($d_{min}$) of 1.6 Å and on a native rTp32 crystal ($d_{min}$ = 1.85 Å). Statistics on the crystallographic data are found in Table I. Phases for the protein were obtained by the single-anomalous dispersion (SAD) method with the program Solve (20) using data collected on the SeMet variant of rTp32 at a wavelength corresponding to the absorption maximum of selenium. The resolution range used was 19.84–2.00 Å. The program identified five selenium sites, and the initial phases had a figure of merit of 0.50. An initial model was constructed automatically using the program Resolve (21, 22) and completed manually with the program O (23). At this stage, electron density for a bound L-selenomethionine was clearly present at the interface between the two domains in Tp32. Refinement of the model utilized data from the aforementioned native crystal of rTp32. The native data showed corresponding electron density for a bound L-methionine. The model was refined using the simulated-annealing, conjugate-gradient minimization, and individual B-factor refinement protocols available in CNS version 1.1 (24). Alternate conformations for several residues were modeled, and their occupancies were refined. The model was adjusted using O and XtalView (25). Solvent molecules were added after the protein part was complete and where chemically reasonable. The final model includes residues 5–244 of rTp32 and a single, non-covalently bound molecule of L-methionine. Table I shows the refinement statistics. Automated searches for structurally related proteins were carried out using the DALI server (26). The strongest similarity (Z = 18.5, where Z > 2 is considered to be similar) was between rTp32 and the hypothetical protein pg110 fragment. When an individual domain of the protein was used as the basis of the search, similarities to several members of the periplasmic protein binding-like superfamily, as defined by the Structural Classification of Proteins, were apparent (27). For example, domain II of rTp32 (see below) had a Z score of 12.2 when compared with one of the domains of the lysine-, arginine-, and ornithine-binding protein.

TABLE I
*Data collection, phasing, and refinement statistics.*

| Structure | Native | SeMet |
|---|---|---|
| Space group | $P2_12_12$ | $P2_12_12$ |
| *a* | 96.248 | 95.893 |
| *b* | 46.404 | 46.348 |
| *c* | 55.217 | 55.154 |
| Resolution, Å[a] | 35.5–1.85 (1.88–1.85) | 50–1.65 (1.68–1.65) |
| No. reflections | 87,097 (2474) | 373,993 (11744) |
| Unique reflections (F > 0) | 38,697 (907) | 56,743 (2717) |
| Completeness, % | 98.1 (87.7) | 99.2 (94.1) |
| Avg. redundancy | 4.0 (2.7) | 6.6 (4.3) |
| Avg. $I/\sigma$ | 17.0 (1.9) | 40.8 (4.1) |
| $R_{sym}$[b] | 0.070 (0.553) | 0.054 (0.349) |
| Refinement Statistics | | |
| Resolution, Å | 35.5–1.85 (1.97–1.85) | |
| No. protein atoms | 1863 | |
| No. L-methionines | 1 | |
| No. waters | 216 | |
| $R_{work}$[c] | 0.187 (0.272) | |
| $R_{free}$[d] | 0.232 (0.312) | |
| R.m.s. deviations | | |
| Bond lengths, Å | 0.013 | |
| Bond angles, ° | 1.6 | |
| Ramachandran distribution[e] | | |
| Favored, % | 94.8 | |
| Allowed, % | 100 | |

[a] Numbers in parentheses are for the highest resolution shell of the data.

[b] $R_{sym} = \Sigma_i|\hat{I}(h) - I_i(h)| / \Sigma_h\Sigma_i I_i(h)$, where $I_i(h)$ is the ith measurement of the intensity for Miller indices h and $\hat{I}(h)$ represents the mean intensity value of the symmetry (or Friedel) equivalent reflections of Miller indices h.

[c] $R_{work} = \Sigma_h||F_{obs}| - |F_{calc}||/\Sigma_h|F_{obs}|$.

[d] The formula for $R_{free}$ is the same as that for $R_{work}$, except it is calculated with a portion of the structure factors (7%, in this case) that had not been used for refinement.

[e] Using a modified Ramachandran plot (45).

## RESULTS AND DISCUSSION

*Biophysical Characteristics of Purified rTp32*—Recombinant Tp32 was created as a non-acylated fusion protein with an N-terminal $His_6$ tag and spacer residues totaling 28 amino acids. The expression of this fusion protein in *E. coli* resulted in the production of soluble protein. Typical yields for purifications were 20–25 mg per liter of culture (>95% pure protein). Upon storage overnight at 4 °C in 20 mM Hepes (pH 7.5), 100 mM NaCl, 15 mM β-mercaptoethanol, recombinant rTp32 precipitated. The precipitate was solubilized by the addition of 2 mM octyl-β-glucoside, followed by incubation for 12 h at room temperature. Size-exclusion chromatography revealed that re-solubilized rTp32 was conformationally homogeneous; re-solubilized rTp32 eluted from the column as a single peak with a calculated molecular mass of about 26 kDa. This is in close agreement with the mass determined by ESI-MS (27,464 Da), indicating that the recombinant protein behaved as a monomer in solution. However, the expected mass, based on the sequence of our construct, of rTp32 (30,155 Da) is 2,691 Da higher than

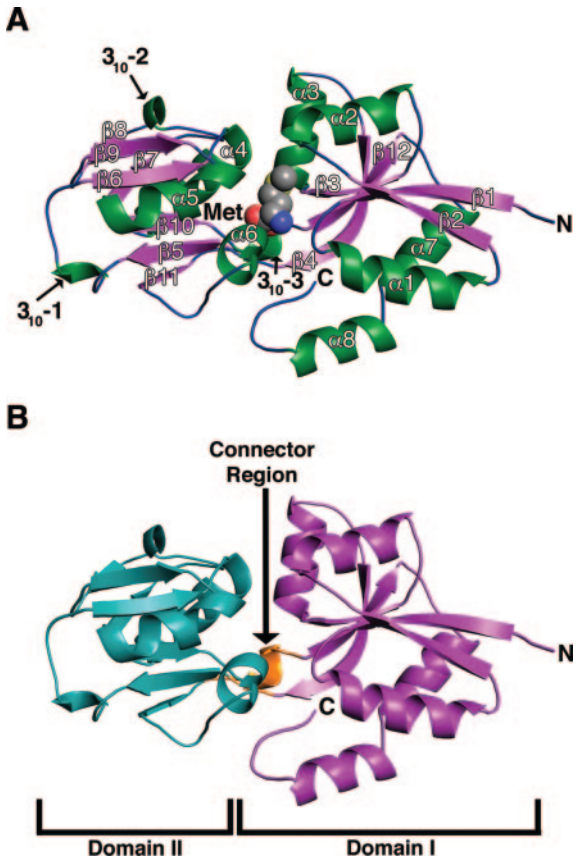


FIG. 1. **The crystal structure of rTp32.** *A*, secondary structure. Shown is a schematic representation of the C$\alpha$ trace of rTp32. Helices are shown in *green*, $\beta$-strands in *purple*, and loop regions in *blue*. The spheres represent the molecule of bound L-methionine. Carbon atoms are colored *gray*, nitrogen *blue*, oxygens *red*, and sulfur *yellow*. *B*, domain structure of rTp32. Domain I is shown in *purple*, Domain II in *cyan*, and the Connector Region is in *orange*. This figure and Fig. 5 were generated using PyMOL and rendered using POV-Ray (www.povray.org).

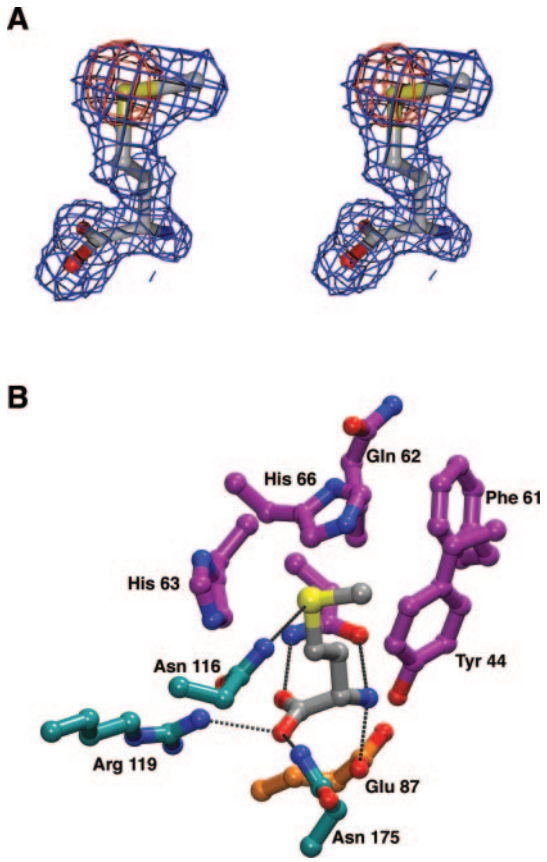


FIG. 2. **Methionine binding to rTp32.** *A*, stereo representation of the electron density for the bound L-methionine. The electron density is superposed on the final model coordinates for the amino acid. The *blue* density is a $2F_o - F_c$ map contoured at the 1$\sigma$ level. The *red* density, contoured at the 20$\sigma$ level, is an anomalous difference Fourier map calculated with phases from the model. The same coloring scheme as in Fig. 1 is used for the atoms. This part of the figure was generated using XtalView and POV-Ray. *B*, methionine binding site. The same coloring scheme used in Fig. 1 is used here, with the following exceptions: carbons from Domain I are *purple*, those from Domain II are *cyan*, and those from the Connector Region are *orange*. Hydrogen bonds are shown as *dashed lines*. Residues shown in this figure that do not participate in hydrogen bonds to the methionine are making van der Waals contacts to the amino acid. Residues making only van der Waals contacts to the main-chain portion of the amino acid are not shown. This part of the figure and Fig. 7 were generated using VMD (44).

the experimentally derived mass of the purified protein. N-terminal sequencing confirmed that the first 21 of 28 vector-derived amino acid residues of rTp32 had been proteolyzed. The $^{1}H$-$^{15}N$ heteronuclear single quantum coherence (HSQC) spectrum of rTp32 exhibited good peak dispersion and uniform intensity (see Fig. 3), indicating that rTp32 was well folded and suitable for crystallization.

*Crystal Structure of rTp32*—To glean possible insights into the function of rTp32, we determined its crystal structure at a resolution of 1.85 Å. rTp32 contains two domains exhibiting a mixed $\alpha/\beta$ structure, with both domains being of similar fold (Fig. 1). The 55 C$\alpha$ atoms from analogous secondary structural elements in the two domains can be superposed with a root-mean-square (r.m.s.) deviation of 1.5 Å. The structure of each domain is comprised of a central core, which consists of a five-stranded $\beta$-sheet flanked by $\alpha$-helices on both sides. We term this the "central fold." In each $\beta$-sheet, one strand is anti-parallel. Domain I (residues 5–85 and 202–244) is slightly larger than Domain II (residues 89–194). The central fold of Domain I encompasses five $\beta$-strands and three $\alpha$-helices. In addition to this, Domain I contains two $\alpha$-helices proximal to the C terminus of the protein. Domain II has a small, two-stranded $\beta$-sheet and two small $3_{10}$-helices outside of its central fold. For the purposes of this report, helix $\alpha$5 is considered as one $\alpha$-helix, but a notable feature of this helix is that it is tightly wound at both ends, exhibiting $3_{10}$-helical hydrogen-bonding patterns. The protein contains two linkers between the domains, connector region I (CRI, residues 86–88), and connector region II (CRII, residues 195–201). CRI is devoid of regular secondary structure, but CRII features a small $3_{10}$-helix. The total buried surface area at the interface between the two domains is 1,850 Å$^2$.

*L-Methionine Binding Site*—A molecule of L-methionine was unexpectedly observed within the electron density map, bound non-covalently within a pocket between the two domains (Fig. 2*A*). The identity of this molecule was ascertained using two methods: 1) the size and shape of the electron density was consistent with L-methionine; 2) the selenomethionine variant of rTp32 displays density in an anomalous difference Fourier map at the expected position of a selenium atom in selenomethionine (Fig. 2*A*). Because no amino acids were included in the crystallization medium, we assume the protein-acquired methionine from the cytoplasm of the expression organism (*E. coli*). The binding of L-methionine to rTp32 appears to be specific, because the electron density in the binding pocket displays no evidence of binding by other small molecules, even though all twenty amino acids and a multitude of other small metabolites are present in the *E. coli* cytoplasm. Both domains participate in the binding of the L-methionine (Fig. 2*B*). The

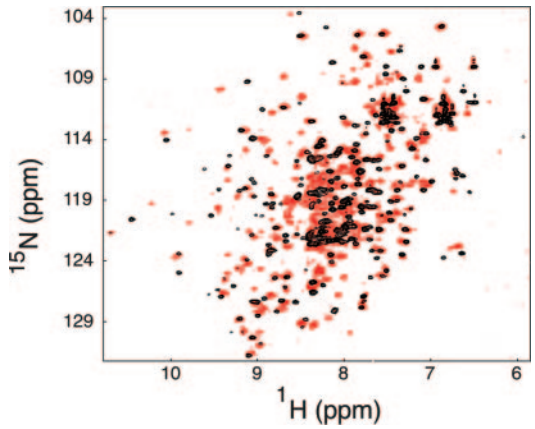


FIG. 3. **Superposition of $^{1}$H-$^{15}$N HSQC spectra of rTp32 in the holo (*black*) and apo (*red*) forms.**

pocket may be divided into two sections, main-chain binding and side-chain binding. The chemical character of these parts is well suited to binding an L-methionine, which, at physiological pH, has charged amino and carboxylate moieties and a mostly hydrophobic side chain. The main chain binding portion of the pocket is lined with polar and charged residues; these side chains engage in hydrogen bonds to the amino and carboxylate moieties of the bound L-methionine (Fig. 2*B*). Compensation for the charges on the bound methionine is provided by the charged residues Glu-87 and Arg-119. The side-chain binding side of the pocket harbors a mixture of hydrophobic and polar residues. The hydrophobic residues (Phe-61 and Tyr-44) make van der Waals contacts with the ϵ-methyl group. Most of the polar residues on this side of the pocket do not make hydrogen bonds to the methionine side chain. Rather, they provide further van der Waals contacts to the methionyl moiety (Fig. 2*B*). One polar residue, Asn-116, makes a hydrogen bond via the amide nitrogen atom of its side chain to the δ-sulfur in the methionine side chain.

The amino acid-binding pocket of rTp32 appears to be well suited to specifically bind methionine. During the expression of the protein in the cytoplasm of *E. coli*, L-methionine outcompetes a myriad of other small molecules for binding to the amino acid binding pocket. The L-methionine is tightly bound to the protein. This is evidenced by the fact that the amino acid did not dissociate from rTp32 during several purification procedures in which no exogenous L-methionine was provided. Further buttressing this notion is the observation that only very harsh treatments were capable of removing the bound L-methionine (see below). The reasons for this tight binding are evident from the structure. The shape of the amino acid binding pocket is complementary to that of L-methionine; every atom of the side chain is involved in van der Waals interactions with the protein. Also, the aforementioned hydrogen bond between Asn-116 and the methionyl side chain makes the interaction even more favorable. It would be informative to assess whether other amino acids could bind to this methionine-binding pocket.

Once it was determined that L-methionine was bound to purified rTp32, efforts were undertaken to obtain apoprotein. To this end, the protein was subjected to denaturation in 6 M guanidine hydrochloride, followed by renaturation (see "Experimental Procedures"). rTp32 treated in this manner was then analyzed by NMR. A $^{1}$H-$^{15}$N HSQC spectrum of the apo and methionine-bound states of rTp32 (Fig. 3) revealed that renatured protein underwent significant conformational change, as indicated by peak broadening and an increase in the number of resonances in the random-coil range of the spectrum. In addition, comparative analysis of peak intensities between the native and renatured proteins showed that 20% of the renatured protein retained the L-methionine ligand. The renatured protein is functional, as indicated by the fact that the addition of 1 mM L-methionine to the renatured protein resulted in an HSQC spectrum that was identical to the native, liganded protein (not shown). Given the degree of difficulty in obtaining ligand-free rTp32, further quantitative studies of ligand binding to rTp32 remain technically challenging.

*Comparisons to Other Related Binding Proteins*—An automated search for structurally related proteins reveals that Tp32 is a member of a group of proteins termed the periplasmic binding protein-like superfamily. This superfamily includes other proteins that bind amino acids, such as the lysine-, arginine-, ornithine-binding protein (LAOBP) and the histidine-binding protein (HisJ) (28, 29). Many such proteins function as small-molecule receptor components of ABC transporter systems (30) that utilize ATP to transport small molecules from the external milieu to the cytoplasm. These structural similarities correlate with recent genetic studies suggesting that Tp32 has amino acid sequence homology to a methionine-uptake protein from *E. coli*, called YaeC (31). YaeC is the methionine receptor for a newly discovered ABC transporter family, called the methionine uptake transporter (MUT) family. An amino acid sequence comparison between YaeC and Tp32 shows that the two globular portions of the proteins are about 34% identical. In particular, the residues that are in contact with the methionine are nearly 100% conserved (see below). The only exception is Glu-87 of Tp32. The equivalent position in YaeC is a tyrosine. The ability of rTp32 to bind L-methionine and the high degree of similarity between YaeC and Tp32 prompts us to conclude that the function of Tp32 likely is to serve as the methionine receptor (of a MUT ABC transporter) at the cytoplasmic membrane of *T. pallidum*. The high degree of sequence similarity observed between Tp32 and YaeC extends to all members of the MUT family (Fig. 4). Again, almost all the residues that contact the bound L-methionine are well conserved in this family. The least-conserved methionine-contacting residue is Glu-87. This is due to the fact that at least some members of this family bind methionine-binding peptides (see below). It is unknown whether both stereoisomers of methionine can bind to Tp32. Because *T. pallidum* apparently lacks the methionine racemase for conversion of D to L forms, the ability of this organism to utilize D-methionine is uncertain.

Several other structures of periplasmic ligand-binding proteins (PLBPs) bound with their cognate amino acids are known (29, 32, 33). They are HisJ, LAOBP, and the glutamine-binding protein (QBP). The overall fold of these polypeptides is similar to that of rTp32. In comparing them to rTp32, the positions of the ~140 analogous Cα atoms superpose with r.m.s. deviations of about 1.9 Å in all three cases. An overlay of rTp32 and QBP is shown in Fig. 5. Some significant differences between the two structures, however, exist outside of the central domain folds. In particular, two protrusions from the globular core of QBP are not present in rTp32. Researchers have speculated that these features interact with the membrane-spanning components of the LAOBP, HisJ, and QBP transporters (28, 33). On the opposite faces of the proteins, rTp32 has a protuberance that is absent in QBP (Fig. 5). The protuberance is located between residues 128 and 152, an area of rTp32 that includes the small β-sheet composed of strands β7 and β8, as well as a $3_{10}$-helix ($3_{10}$-2). This feature is proximal to a patch of negative charge on the protein (Fig. 6) (34). The combination of the protuberance and the charge make this area of the protein a prime candidate for the surface that interacts with the unknown membrane-spanning component of the treponemal methionine-transport system.

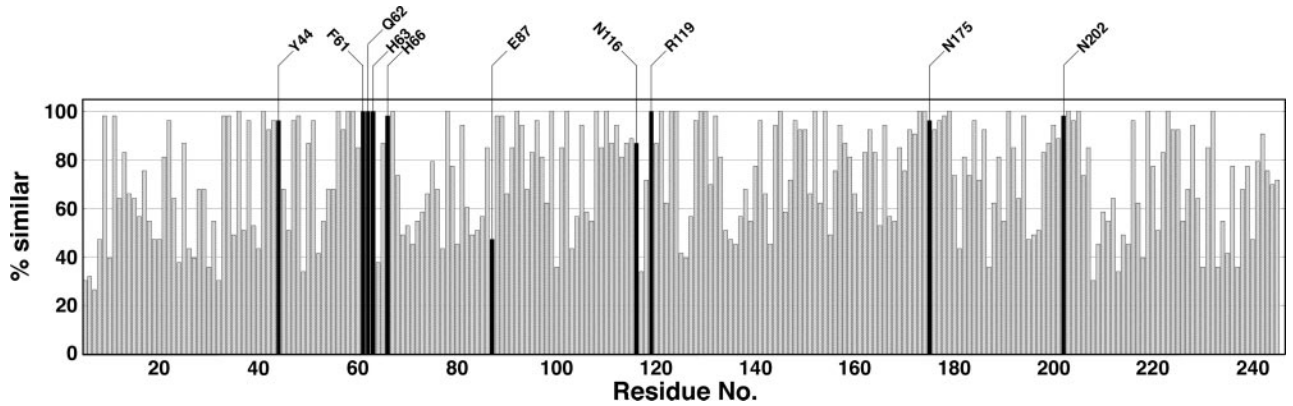


FIG. 4. **Sequence similarity of the MUT family with respect to rTp32.** The *x*-axis of the graph is the residue number of rTp32. The sequence of rTp32 was aligned to those of 52 other MUT family members. The height of the *bars* indicate the percentage of sequences that have residues that are similar to the predominant residue type (hydrophobic, polar, acidic, or basic) at the given sequence position. *Black bars* denote residues that are in contact with L-methionine in the rTp32 structure. The identities of the rTp32 residues at the *black bar* positions are noted at the *top* of the figure.

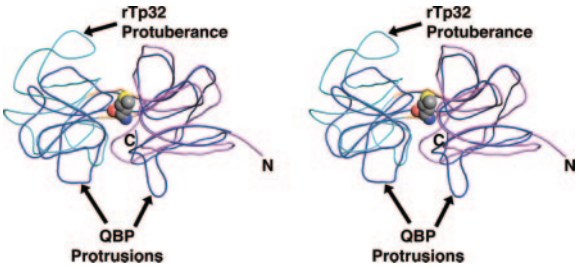


FIG. 5. **Comparison of rTp32 and QBP.** A stereo representation of the smoothed traces for the C$\alpha$ atoms of rTp32 and QBP are shown in their optimal superposition. The trace for QBP is shown in *blue*, and the trace for rTp32 is color-coded as in Fig. 1*B*.

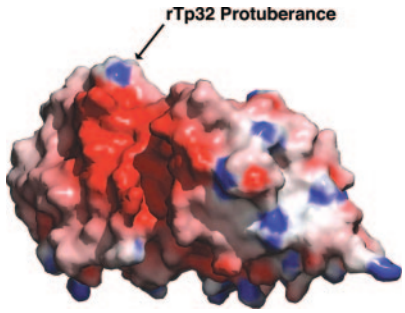


FIG. 6. **Surface features of rTp32.** Areas of negative electrostatic potential are colored *red*, and areas of positive potential are shaded *blue*. The range used for the electrostatic potential was −10 to +10 kT. This figure was generated using GRASP (34).

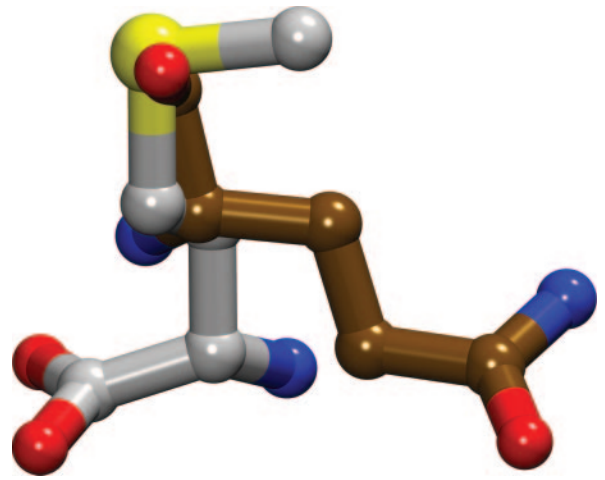

FIG. 7. **Relative orientations of the amino acids bound to rTp32 and QBP.** Shown are the amino acids bound to rTp32 (*gray carbons*) and QBP (*brown carbons*). The two protein structures were superposed without taking these amino acids into account.

Another difference between rTp32 and the other ligand-bound periplasmic binding proteins occurs in the connector regions. In LAOBP, HisJ, and QBP, the respective connector regions either have no regular secondary structure, or they are $\beta$-strands. In rTp32, however, one of the connector regions (CRII) contains a small $3_{10}$-helix ($3_{10}$-3, Fig. 1). This connector region conformation is unique among the members of the family of all PLBPs. The connector regions of some other PLBPs comprise $\alpha$-helices (35) or $\beta$-strands (33), but a $3_{10}$-helix in this region has been observed only in methionine binding components of the MUT family (see below). Comparisons of the liganded and unliganded structures of the other periplasmic amino acid binding proteins show that the two domains undergo large positional changes with respect to one another when substrates bind (28, 33). The presence of helix $3_{10}$-3 may restrict the conformational changes that are available to rTp32. It would therefore be valuable to determine the structure of the apoprotein in order to evaluate the extent of interdomain motion possible in this fold.

The aforementioned superpositions, which were carried out using only the protein C$\alpha$ atoms, illuminate differences between the amino acid binding pocket of rTp32 and those of the other amino acid binding proteins. Most significantly, the L-methionine bound to rTp32 is rotated ~90° relative to the amino acids bound to the other three proteins (Fig. 7). The side chain of the L-methionine adopts the position that the carboxylate moieties occupy in the other structures. The shape of the amino acid binding pocket of rTp32 differs from those of the other amino acid binding proteins, and the positions of charged and hydrophobic moieties within the pocket are also different. These differences result in the contrasting orientation of the bound amino acid.

Structural similarity searches recently revealed that Tp32 has homology with a hypothetical protein pg110 from *Staphylococcus aureus* (Protein Data Bank ID code 1p99). Zhang *et al.* (31) also have proposed that pg110 (BAB56626) protein is a methionine binding member of the MUT family of ABC transporters. The structural similarity between pg110 and rTp32 is marked: the proteins have 244 comparable $C_\alpha$ atoms that, when superposed, have an r.m.s. deviation of only 1.3 Å. Like rTp32, pg110 harbors a $3_{10}$-helix in its connector region. The pg110 protein has an extended C terminus compared with

rTp32. This extension forms a loop and an α-helix that pack on the surface of Domain I. In contrast to rTp32, the pg110 protein appears to bind a Gly-Met dipeptide, rather than a sole L-methionine. The orientation and amino acid-to-protein contacts of the methionine complexed within the amino acid binding pocket of pg110 are very similar to those observed in rTp32, and the amino acid binding pockets of the two proteins are nearly identical. Only two areas of the pocket are different between the two proteins. The first area is in the hydrophobic side-chain binding portion of the pocket, where rTp32 residue His-66, is replaced by a phenylalanine (Phe-97) in gp110. The second area is in the main-chain binding portion of the pocket. rTp32 residue Glu-87, which forms a hydrogen bond to the amino moiety of the bound L-methionine, has been replaced in pg110 with an alanine (Ala-119). In addition, other amino acid differences between the two proteins have the effect of rendering the main-chain binding section of the pocket more capacious in pg110. These changes accommodate the N-terminal residue of the Gly-Met dipeptide. Therefore, it appears that some of the proteins identified by Zhang *et al.* (31) as methionine-binding proteins may also accommodate small methionine-containing peptides. These results suggest that at least part of the reason that Glu-87 of rTp32 is poorly conserved in the MUT methionine-binding proteins (Fig. 4) is because some members may need a smaller amino acid at this position in order to harbor covalent adducts of methionine in the binding pocket.

*Summary and Implications—T. pallidum* is among the few human bacterial pathogens that yet cannot be cultivated *in vitro*. This limitation has severely restricted viable avenues of investigation for elucidating key features of the enigmatic traits of the spirochete, including discerning the functions of its membrane proteins. Although genome sequence analysis has characterized Tp32 as a cell envelope lipoprotein (6), structural data presented herein suggest that Tp32 is a periplasmic methionine-binding protein component of an ABC transporter system. Further structural studies on other treponemal proteins thus are likely to continue to yield important insights into their unknown physiological functions.

Periplasmic binding proteins are important components of the bacterial ABC-type transporter superfamily, which is involved in the transport of various ligands (36, 37). In *E. coli*, genes *abc*, *yaeE*, and *yaeC* comprise a MUT operon (recently renamed as *metNIQ*) that encodes the ATPase, permease, and periplasmic methionine-binding protein, respectively (31, 38, 39). Although MetQ in *E. coli* likely is free within the periplasm (38), as is common for periplasmic receptors in Gram-negative bacteria (40), Tp32, as a lipoprotein, likely is tethered via its lipid moieties to the outer leaflet of the cytoplasmic membrane. This topology would allow the polypeptide to reside within the polar environment of the periplasm, consistent with the observation that rTp32 was highly soluble when its acyl moieties were absent. This proposed membrane architecture in *T. pallidum*, however, is more akin to how Gram-positive bacteria model their surfaces; Gram-positive bacteria exploit the lipids of their lipoproteins as one of two principal mechanisms for anchoring their receptors to their cell surfaces (thereby compensating for the lack of a periplasm) (41). As one might predict from this, orthologs of the Gram-negative *metNIQ* MUT system exist in Gram-positive bacteria (*i.e. metNPQ*) (42). That *T. pallidum*, despite its dual membrane system, displays membrane architectural features that more closely parallel those of Gram-positive rather than Gram-negative bacteria speaks further to the peculiar membrane biology of this enigmatic human pathogen (2, 3, 15).

An analysis of genome sequence information suggests that *T. pallidum* likely encodes 38 transporter proteins, ~60% of which belong to the ABC transporter family (www.biology.ucsd.edu/~msaier/transport/). The capability of *T. pallidum* to synthesize many key metabolites thus appears to have been lost during evolution, culminating in the need to exploit its requisite human host extensively by expressing transport proteins for numerous ligands and metabolites. In this regard, *T. pallidum* appears to lack the genes that would be involved in *de novo* biosynthesis of methionine, with the exception perhaps of MetK (*S*-adenosylmethionine synthetase; TP0794), which converts methionine to *S*-adenosylmethionine, which is important for many intracellular processes (43).

Subsequent to our determination of the structure of Tp32, Zhang *et al.* (31) proposed that the *T. pallidum* genes TP0120, TP0119, TP0821 (Tp32) were orthologs of *E. coli* MetN, MetI, and MetQ, respectively, and thus likely were members of the MUT family. However, unlike most other ABC-like transport systems, which tend to cluster as operons (31), the three aforementioned treponemal genes are not contiguous, nor are the gene arrangements adjacent to *tp32* consistent with *tp32* comprising any other type of operon (6). Nonetheless, Tp32 as the methionine-binding protein likely interacts with TP0120 (ATPase) and TP0119 (permease) to deliver methionine to the cytoplasm of *T. pallidum*. Although these putative protein-protein interactions remain to be established, the negatively charged surface of Tp32 adjacent to a pronounced protein protuberance (Figs. 5 and 6) may be critical for interaction with cognate permease (*i.e.* TP0119). Further crystallographic studies of the treponemal MUT system in the methionine-trapped state may reveal the interactions and conformational changes that accompany ligand transport, ATP binding, and hydrolysis associated with methionine transport in *T. pallidum*. Nonetheless, our crystal structure data support the notion that Tp32 is an ortholog of *E. coli* MetQ, and therefore Tp32 is a *bona fide* member of the MUT family (31).

*Acknowledgments*—We thank Patrick Conley and Sandra Hill for technical assistance, Kevin Gardner for advice and guidance, Bikash Pramanik for mass spectrometry, Carson Harrod for reviewing the manuscript, and Andrzej Joachimiak and the staff of the Structural Biology 19-ID beamline for expert aid in data collection.

REFERENCES

1. Norris, S. J. (1993) *Microbiol. Rev.* **57,** 750–779
2. Radolf, J. D. (1994) *Trends Microbiol.* **2,** 307–311
3. Radolf, J. D. (1995) *Mol. Microbiol.* **16,** 1067–1073
4. Chamberlain, N. R., Brandt, M. E., Erwin, A. L., Radolf, J. D., and Norgard, M. V. (1989) *Infect. Immun.* **57,** 2872–2877
5. Haake, D. A. (2000) *Microbiology* **146,** 1491–1504
6. Fraser, C. M., Norris, S. J., Weinstock, G. M., White, O., Sutton, G. G., Dodson, R., Gwinn, M., Hickey, E. K., Clayton, R., Ketchum, K. A., Sodergren, E., Hardham, J. M., McLeod, M. P., Salzberg, S., Peterson, J., Khalak, H., Richardson, D., Howell, J. K., Chidambaram, M., Utterback, T., McDonald, L., Artiach, P., Bowman, C., Cotton, M. D., Fujii, C., Garland, S., Hatch, B., Horst, K., Roberts, K., Sandusky, M., Weidman, J., Smith, H. O., and Venter, J. C. (1998) *Science* **281,** 375–388
7. Hayashi, S., and Wu, H. C. (1990) *J. Bioenerget. Biomem.* **22,** 451–471
8. Sutcliff, I. C., and Russell, R. R. B. (1995) *J. Bacteriol.* **177,** 1123–1128
9. Becker, P. S., Akins, D. R., Radolf, J. D., and Norgard, M. V. (1994) *Infect. Immun.* **62,** 1381–1391
10. Steere, A. C., Sikand, V. K., Meurice, F., Parenti, D. L., Fikrig, E., Schoen, R. T., Nowakowski, J., Schmid, C. H., Laukamp, S., Buscarino, C., Krause, D. S., and The Lyme Disease Vaccine Study Group (1998) *N. Engl. J. Med.* **339,** 209–215
11. Ochsner, U. A., Vasil, A. I., Johnson, Z., and Vasil, M. L. (1999) *J. Bacteriol.* **181,** 1099–1109
12. Radolf, J. D., Arndt, L. L., Akins, D. R., Curetty, L. L., Levi, M. E., Shen, Y., Davis, L. S., and Norgard, M. V. (1995) *J. Immunol.* **154,** 2866–2877
13. Norgard, M. V., Arndt, L. L., Akins, D. R., Curetty, L. L., Harrich, D. A., and Radolf, J. D. (1996) *Infect. Immun.* **64,** 3845–3852
14. Deka, R. K., Goldberg, M. S., Hagman, K. E., and Norgard, M. V. (2004) *J. Bacteriol.* **186,** 2303–2308
15. Cox, D. L., Chang, P., McDowall, A., and Radolf, J. D. (1992) *Infect. Immun.* **60,** 1076–1083
16. Pace, C. N., Vajdos, F., Fee, L., Grimsley, G., and Gray, T. (1995) *Prot. Sci.* **4,** 2411–2423
17. Delaglio, F., Grzesiek, S., Vuister, G. W., Zhu, G., Pfeifer, J., and Bax, A. (1995) *J. Biomol. NMR* **6,** 277–293

18. Johnson, B. A., and Blevins, R. A. (1994) *J. Biomol. NMR* **4,** 603–614
19. Otwinowski, Z., and Minor, W. (1997) *Methods Enzymol.* **276,** 307–326
20. Terwilliger, T. C., and Berendzen, J. (1999) *Acta Crystallogr. Sect. D* **55,** 849–861
21. Terwilliger, T. C. (2002) *Acta Crystallogr. Sect. D* **58,** 2213–2215
22. Terwilliger, T. C. (2003) *Acta Crystallogr. Sect. D* **59,** 38–44
23. Jones, T. A., Zou, J. Y., Cowan, S. W., and Kjeldgaard, M. (1991) *Acta Crystallogr. Sect. A* **47,** 110–119
24. Brunger, A. T., Adams, P. D., Clore, G. M., DeLano, W. L., Gros, P., Grosse-Kunstleve, R. W., Jiang, J. S., Kuszewski, J., Nilges, M., Pannu, N. S., Read, R. J., Rice, L. M., Simonson, T., and Warren, G. L. (1998) *Acta Crystallogr. Sect. D* **54,** 905–921
25. McRee, D. E. (1992) *J. Mol. Graph.* **10,** 44–46
26. Holm, L., and Sander, C. (1994) *Proteins* **19,** 165–173
27. Murzin, A. G., Brenner, S. E., Hubbard, T., and Chothia, C. (1995) *J. Mol. Biol.* **247,** 536–540
28. Oh, B.-H., Pandit, J., Kang, C.-H., Nikaido, K., Gokcen, S., Ames, G. F.-L., and Kim, S.-H. (1993) *J. Biol. Chem.* **268,** 11348–11355
29. Yao, N., Trakhanov, S., and Quiocho, F. A. (1994) *Biochemistry* **33,** 4769–4779
30. Nikaido, H., and Hall, J. A. (1998) *Methods Enzymol.* **292,** 3–20
31. Zhang, Z., Feige, J. N., Chang, A. B., Anderson, I. J., Brodianski, V. M., Vitreschak, A. G., Gelfand, M. S., and Saier, M. H. (2003) *Arch. Microbiol.* **180,** 88–100
32. Oh, B.-H., Ames, G. F.-L., and Kim, S. H. (1994) *J. Biol. Chem.* **269,** 26323–26330
33. Sun, Y.-J., Rose, J., Wang, B.-C., and Hsiao, C.-D. (1998) *J. Mol. Biol.* **278,** 219–229
34. Nicholls, A., Sharp, K. A., and Honig, B. (1991) *Proteins* **11,** 281–296
35. Lee, Y.-H., Deka, R. K., Norgard, M. V., Radolf, J. D., and Hasemann, C. A. (1999) *Nat. Struct. Biol.* **6,** 628–633
36. Davidson, A. L., and Chen, J. (2004) *Annu. Rev. Biochem.* **73,** 241–268
37. Higgins, C. F. (2001) *Res. Microbiol.* **152,** 205–210
38. Merlin, C., Gardiner, G., Durand, S., and Masters, M. (2002) *J. Bacteriol.* **184,** 5513–5517
39. Gal, J., Szvetnik, A., Schnell, R., and Kalman, M. (2002) *J. Bacteriol.* **184,** 4930–4932
40. Oliver, D. B. (1996) in *Escherichia coli and Salmonella Cellular and Molecular Biology* (Neidhardt, F. C., ed) pp. 88–103, ASM Press, Washington, D. C.
41. Navarre, W. W., and Schneewind, O. (1999) *Microbiol. Mol. Biol. Rev.* **63,** 174–229
42. Hullo, M. -F., Auger, S., Dassa, E., Danchin, A., and Martin-Verstraete, I. (2004) *Res. Microbiol.* **155,** 80–86
43. Rodionov, D. A., Vitreschak, A. G., Mironov, A. A., and Gelfand, M. S. (2004) *Nucleic Acids Res.* **32,** 3340–3353
44. Humphrey, W., Dalke, A., and Schulten, K. (1996) *J. Mol. Graph.* **14,** 33–38
45. Lovell, S. C., Davis, I. W., Arendall, W. B., de Bakker, P. I., Word, J. M., Prisant, M. G., Richardson, J. S., and Richardson, D. C. (2003) *Proteins* **50,** 437–450